Optimization and Prediction in Natural Gas Networks Using Graph Neural Networks and MPCC-Based Models

Cristian Alejandro Blanco Martínez

Universidad Tecnológica de Pereira
Grupo de investigación Automática

August 14, 2025

Energy Context & Relevance of Natural Gas

Natural gas plays a crucial role in the global energy mix, offering a cleaner alternative to other fossil fuels by producing lower CO_2 emissions. It supports both industrial processes and electricity generation, acting as a reliable energy source in diverse contexts.

In Colombia, natural gas is widely used across the residential, commercial, industrial, and thermal power sectors. Its importance becomes evident during dry seasons, when hydroelectric generation is reduced and thermal plants, fueled by natural gas, step in to maintain electricity supply.

Operational Challenge in the Colombian Energy System

Colombia's electricity supply relies heavily on hydroelectric plants, which are highly dependent on rainfall patterns. During dry seasons, reduced water availability forces the system to increase the participation of thermal plants powered by natural gas.
This seasonal shift places significant operational stress on the gas transport network.

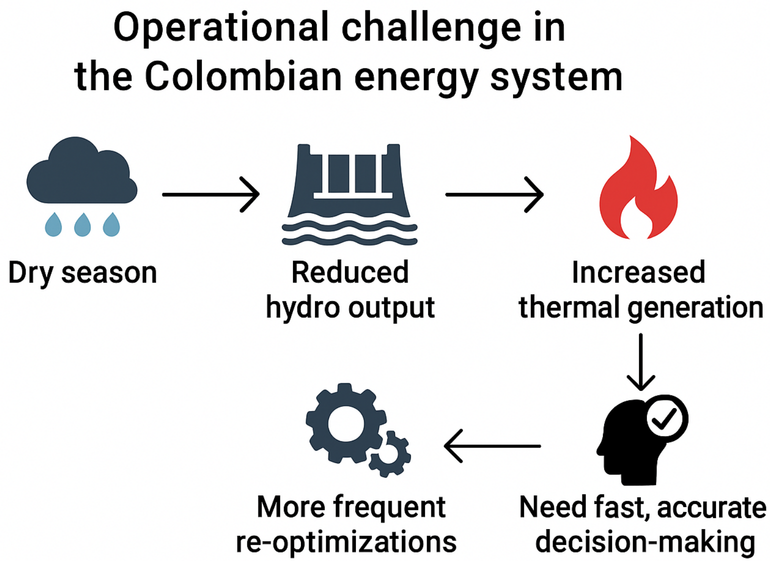

Motivation & Problem Statement

- **Large-scale natural gas networks** require solving complex optimization problems.
- Classical approaches are accurate but often **computationally expensive**.
- Increasing network size and operational constraints lead to:
  - Long execution times
  - Difficulty in real-time or near real-time decision making
- Need for approaches that **preserve accuracy while reducing computation time**.

Objectives

General Objective:

- Develop an optimization tool that integrates knowledge of the gas transportation network topology, a suitable approximation of the Weymouth equation and stochastic optimization techniques to address the gas transportation task taking into account the uncertainties related to hydroelectric generation and the growth of alternative energy sources.

Objectives

Specific Objectives:

- Design a Graph Neural Networks-based approach of regression that integrates knowledge of natural gas network topology to reduce computational time for operation estimation.
- Develop an optimization model for natural gas transportation systems that takes into account the Weymouth equation for reducing that reduces the approximation error in pipeline gas flow calculations.
- Develop a stochastic gas flow dispatch optimization strategy that quantifies the uncertainty in the objective variables and decision variables associated with the operation of the gas system taking into account the constraints of the transportation problem.

Natural Gas System Prediction Using Graph Neural Networks

- Traditional optimizers are **accurate but slow** for large-scale or real-time scenarios.
- Gas networks are inherently **graphs**: nodes = wells, users, storage; edges = pipelines, compressors.
- GNNs exploit **topology-aware learning** for faster prediction.
- **Goal:** Achieve near-optimizer accuracy with runtime reduction.

CensNet Layers: Integrating Node & Edge Features

Motivation: Traditional GCNs focus mainly on *node features* and ignore *edge features*, missing part of the graph's information.

CensNet innovation:

- Alternates between **node layers** and **edge layers**.
- Each layer type updates its own features while using information from the other:
  - **Node layer:** Node embeddings are updated using both node adjacency and transformed edge features.
  - **Edge layer:** Edge embeddings are updated using edge adjacency and transformed node features.
- Uses an *incidence matrix* $\mathbf{T}$ to switch between node and edge domains.

Benefits:

- Captures both *structural* (adjacency) and *relational* (edge) information.
- Enhances long-range dependencies through alternating propagation.

Mathematical Structure of CensNet Layers

Node layer propagation:

$$\mathbf{H}_v^{(l+1)} = \sigma\left(\mathbf{T}\Phi(\mathbf{H}_e^{(l)}\mathbf{p}_e)\mathbf{T}^\top \odot \tilde{\mathbf{A}}_v\mathbf{H}_v^{(l)}\mathbf{W}_v\right)$$

Edge layer propagation:

$$\mathbf{H}_e^{(l+1)} = \sigma\left(\mathbf{T}^\top\Phi(\mathbf{H}_v^{(l)}\mathbf{p}_v)\mathbf{T} \odot \tilde{\mathbf{A}}_e\mathbf{H}_e^{(l)}\mathbf{W}_e\right)$$

Key components:

- $\tilde{\mathbf{A}}_v, \tilde{\mathbf{A}}_e$: normalized adjacency matrices (nodes/edges).
- $\mathbf{T}$: incidence matrix mapping between node and edge domains.
- $\Phi(\cdot)$: diagonal scaling from projected features.
- $\odot$: element-wise filtering of adjacency by feature-derived weights.

Core idea: Information “switches” between node and edge spaces at each step, enriching representations.

CensNet-based Model Architecture

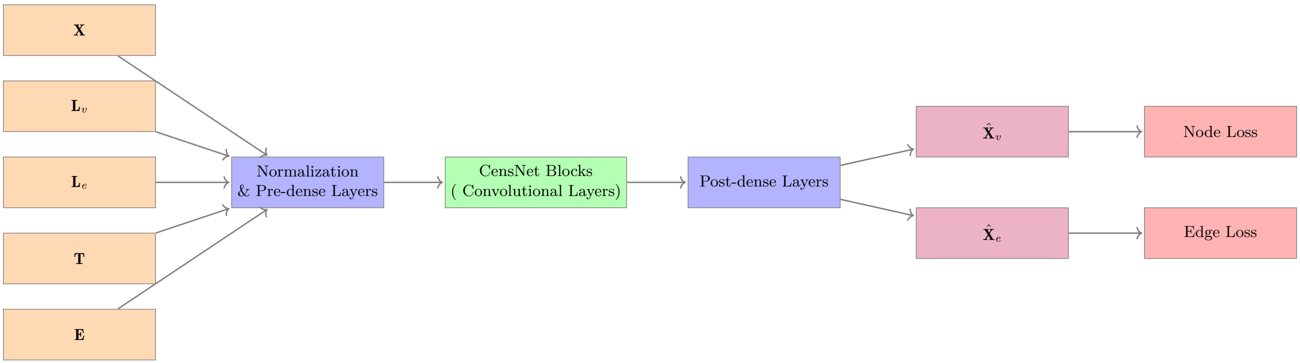

Inputs: Encapsulate both physical attributes and topological information of the gas network:

- Node features ($\mathbf{X}$): pressures, injections, withdrawals, demand forecasts.
- Node Laplacian ($\mathbf{L}_v$) and Edge Laplacian ($\mathbf{L}_e$): encode structural connectivity and enable topology-aware learning.
- Edge features ($\mathbf{E}$): capacities, compressor ratios.
- Incidence matrix ($\mathbf{T}$): explicit mapping between nodes and edges.

CensNet-based Model Architecture

- **Processing:**
  - Normalization and pre-dense layers transform inputs into a common latent space.
  - *CensNet convolutional blocks* perform message passing on both node and edge domains, enabling simultaneous learning of flow patterns and interactions.
  - Post-dense layers refine features for prediction.
- **Outputs:**
  - Node-level injected flows ($\hat{\mathbf{X}}_v$) — predicted gas supply/demand at each node.
  - Edge-level transported flows ($\hat{\mathbf{X}}_e$) — predicted flow rates in each pipeline.

CensNet-based Model Architecture

- **Training:** Node and edge predictions are penalized separately using task-specific loss terms, ensuring both accuracy and physical consistency. For regression tasks, the model minimizes a regularized MSE loss:

$$\mathcal{L}(\Theta) = \sum_{r=1}^{R} \| Y_r - \hat{Y}_r \|_2^2 + \lambda \|\Theta\|_p$$

  where Y_r and $\hat{Y}_r$ are target and predicted values for task r, and $\lambda\|\Theta\|_p$ is a regularization term to prevent overfitting.

Optimization Problem: Objective and Constraints

The gas network consists of wells $\mathcal{W}$ (supply nodes), users $\mathcal{U}$ (demand nodes), pipelines $\mathcal{P}$, and compressors $\mathcal{C}$.

$$\min_{\mathcal{P},\mathcal{F}} \sum_{t\in\mathcal{T}} \left(\sum_{w\in\mathcal{W}} C_w f_w + \sum_{p\in\mathcal{P}} C_p f_p + \sum_{c\in\mathcal{C}} C_c f_c + \sum_{u\in\mathcal{U}} C_u f_u \right)$$

where C_i is the cost per unit flow at element i, and f_i is the corresponding gas flow.

$$\underline{f_w} \le f_w \le \overline{f_w} \quad \forall\ w \in \mathcal{W} \qquad \text{Well capacity} \tag{1}$$

$$-\overline{f_p} \le f_p \le \overline{f_p} \quad \forall\ p \in \mathcal{P} \qquad \text{Pipeline limits} \tag{2}$$

$$0 \le f_u \le \overline{f_u} \quad \forall\ u \in \mathcal{U} \qquad \text{Demand satisfaction} \tag{3}$$

$$\sum_{m:(m,n)\in\mathcal{A}} f_m = \sum_{m':(n,m')\in\mathcal{A}} f_{m'} \qquad \text{Nodal gas balance} \tag{4}$$

Dataset

Two different gas network configurations were used to evaluate the proposed CensNet-based model. The first is a small synthetic case for controlled experimentation, while the second corresponds to the real Colombian natural gas transportation system.

Case	**Nodes**	**Pipelines**	**Compressors**	**Users**
Small Network	8	6	2	2
Colombian Network	63	48	14	27

Table 1: Characteristics of the datasets used.

Experimental Setup

Different network operation scenarios were generated by adding 5%–25% noise to user demand values and solving each scenario with the linear constrained optimization model using APOPT (via GEKKO). The outputs served as ground truth for CensNet model training.

- **Data split:** 60% training, 20% validation, 20% testing.
- **Samples:** 2000 (8-node network), 2400 (63-node network).
- **Training:** 1500 epochs, Adam optimizer, Leaky ReLU activation ($\alpha = 0.2$).
- **Learning rate:** Initial 1×10^{-2}, exponential decay (rate 0.9, steps 1000).
- **Hyperparameters:**
  - N_{channels}: 16–64
  - N_{layers}: 1–5 (CensNet convolutional)
  - N_{dense}: 2–32 (post-dense layers)
- **Losses tested:**
  - Nodal loss only
  - Nodal + Edge loss

Main Results: Prediction Accuracy

Networks: 8-node (synthetic) and 63-node (Colombian gas system)
Models: CensNet (N) – nodal loss only, CensNet (N+E) – nodal + edge loss

- **Nodal flow predictions:** High R^2 in both settings
  - 8-node: $R^2 = 0.988$ (N), 0.988 (N+E)
  - 63-node: $R^2 = 0.996$ (N), 0.996 (N+E)
- **Edge flow predictions:**
  - (N) performs poorly on edges: R^2 low
  - (N+E) improves dramatically: R^2 up to 0.999 (8-node) and 0.996 (63-node)
- **Key takeaway:** Including edge loss is essential for accurate pipeline/compressor flow prediction.

Main Results: Gas Balance & Speed

Gas balance consistency (APOPT – CensNet differences):

- **8-node:** Edge error reduced from 62.92 (N) $\rightarrow$ 39.24 (N+E)
- **63-node:** Edge error reduced from 62.47 (N) $\rightarrow$ -0.07 (N+E)
- Nodal differences < 0.1 units in all cases

Prediction speed: T-tests confirm **CensNet is significantly faster** than APOPT

- 8-node: $T = 14.94$, $p = 1.32 \times 10^{-34}$
- 63-node: $T = 47.29$, $p = 4.92 \times 10^{-110}$

Summary:

- Comparable accuracy to optimization model
- Better edge prediction with (N+E)
- Substantial speed advantage

Interconnected system - Definition

A power-gas interconnected system is a hybrid infrastructure that integrates natural gas and power networks, enhancing overall system efficiency [Duan et al., 2022]. Its key components include power generators, transmission lines, consumption buses, gas wells, pipelines, compressor stations, gas storage units, and consumption nodes.

Objective function

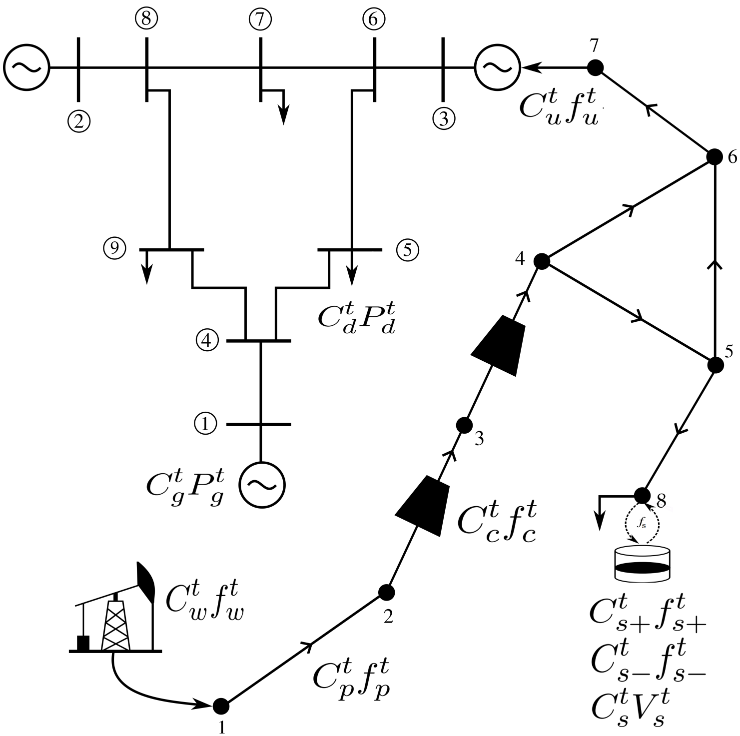

$$
\begin{aligned}
\min_{\mathcal{P},\mathcal{F}} \quad & \sum_{g\in\mathcal{G}} C_g^t P_g^t + \sum_{d\in\mathcal{D}} C_d^t P_d^t + \\
& \sum_{w\in\mathcal{W}} C_w^t f_w^t + \sum_{p\in\mathcal{P}} C_p^t f_p^t + \\
& \sum_{c\in\mathcal{C}} C_c^t f_c^t + \sum_{u\in\mathcal{U}} C_u^t f_u^t + \\
& \sum_{s\in\mathcal{S}} C_{s+}^t f_{s+}^t + \sum_{s\in\mathcal{S}} C_{s-}^t f_{s-}^t + \\
& \sum_{s\in\mathcal{S}} C_s^t V_s^t
\end{aligned}
\tag{5}
$$

Power system constraints

The constraints of the electrical system represent the technical limits of the different elements that compose it, as well as the physical laws that govern it. For certain applications, the DC model is sufficient [Yang et al., 2019].

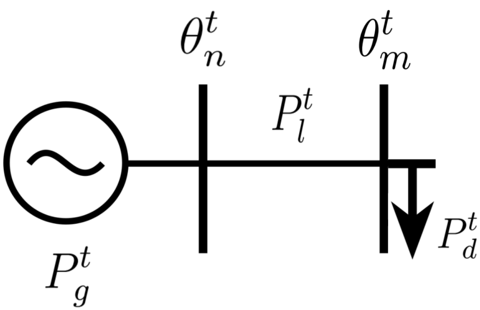

$$
\begin{aligned}
\underline{P_g^t} \leq P_g^t &\leq \overline{P_g^t} && \forall\ g \in \mathcal{G}, && \text{(6a)}\\
-\overline{P_l^t} \leq P_l^t &\leq \overline{P_l^t} && \forall\ l \in \mathcal{L}, && \text{(6b)}\\
P_l^t &= B_{nm}(\theta_n - \theta_m) && \forall\ l = (n, m) \in \mathcal{L}, && \text{(6c)}\\
0 \leq P_d^t &\leq \overline{P_d^t} && \forall\ d \in \mathcal{D}, && \text{(6d)}\\
-\overline{\theta_n^t} \leq \theta_m^t &\leq \overline{\theta_n^t} && \forall\ n \in \mathcal{N}_P, && \text{(6e)}\\
\sum_{\substack{l \in \mathcal{L}_{n+} \\ g=n}} P_l^t + P_g^t &= \sum_{\substack{l \in \mathcal{L}_{n-} \\ d=n}} P_l^t + P_d^t && \forall\ n \in \mathcal{N}_P && \text{(6f)}
\end{aligned}
$$

Interconnection constraints

The second set of restrictions interconnects the natural gas and electric power systems through gas-fired power plants that generate electricity. f_n^t stands for the natural gas fuel consumption to generate a power P_n^t at generator bus $n \in \mathcal{N}_I$, the heat-rate HR_n defines the generator efficiency, and the set $\mathcal{N}_I = \mathcal{G} \cap \mathcal{U}$ holds all the units in the interconnected system belonging to both the power generator and gas demand sets.

$$f_n^t = P_n^t \cdot \mathrm{HR}_n, \quad \forall\ n \in \mathcal{N}_I, \tag{7}$$

Gas system constraints

This set of constraints ensures that wells, pipelines, nodal pressures, compressors, unsupplied demand and storage facilities operate within proper operating limits. [García-Marín et al., 2022].

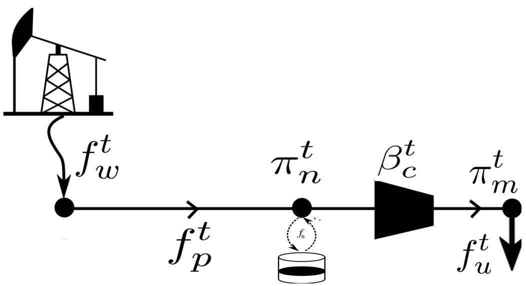

$$\underline{f_w^t} \leq f_w^t \leq \overline{f_w^t} \quad \forall\ w \in \mathcal{W} \tag{8a}$$

$$-\overline{f_p^t} \leq f_p^t \leq \overline{f_p^t} \quad \forall\ p \in \mathcal{P} \tag{8b}$$

$$\underline{\pi_n^t} \leq \pi_n^t \leq \overline{\pi_n^t} \quad \forall\ n \in \mathcal{N}_f \tag{8c}$$

$$\pi_m^t \leq \beta_c^t \pi_n^t \quad \forall\ c = (n, m) \in \mathcal{C} \tag{8d}$$

$$0 \leq f_u^t \leq \overline{f_u^t} \quad \forall\ u \in \mathcal{U} \tag{8e}$$

$$0 \leq f_{s+}^t \leq V_{0s} - \underline{V_s} \quad \forall\ s \in \mathcal{S} \tag{8f}$$

$$0 \leq f_{s-}^t \leq \overline{V_s} - V_{0s} \quad \forall\ s \in \mathcal{S} \tag{8g}$$

$$V_s^t = V_s^{t-1} + f_{s-}^{t-1} - f_{s+}^{t-1} \quad \forall\ s \in \mathcal{S} \tag{8h}$$

Gas system constraints

The gas balance constraints guarantee that the amount of gas entering a node equals the amount leaving it. On the other hand, the Weymouth equation encapsulates the complex physics of gas flow through pipelines between flow rates and pressures.

$$\sum_{m:(m,n)\in\mathcal{A}} f_m^t = \sum_{m':(n,m')\in\mathcal{A}} f_{m'}^t \quad \forall\ n \in \mathcal{N}_f \tag{9a}$$

$$\operatorname{sgn}(f_p^t)(f_p^t)^2 = K_{nm}((\pi_n^t)^2 - (\pi_m^t)^2) \quad \forall\ p = (n,m) \in \mathcal{P} \tag{9b}$$

Modeling this equation as a nonconvex and discontinuous equality constraint poses significant challenges for optimization algorithms. Specifically, the nonconvexity leads to multiple local optima, making it difficult to find the global optimum [Jiang et al., 2021].

Proposed complementarity-based approach

Complementarity constraints can be used to represent non-uniform or discontinuous operators, such as absolute value, sign, and min/max [Baumrucker et al., 2008].

$$y = sgn(f_T^t) \tag{10}$$

The sign equation can be represented by an optimization problem whose constraints avoid the use of binary variables.

$$\mathcal{O}_W: \min_{y_p^t} -y_p^t f_p^t \tag{11a}$$
$$\text{s.t. } y_p^t (f_p^t)^2 = K_{nm}((\pi_n^t)^2 - (\pi_m^t)^2) \tag{11b}$$
$$-1 \leq y_p^t \leq 1 \tag{11c}$$
$$f_p^t = f_{p+}^t - f_{p-}^t \tag{11d}$$
$$0 \leq f_{p+}^t \perp (y_p^t + 1) \geq 0 \tag{11e}$$
$$0 \leq f_{p-}^t \perp (1 - y_p^t) \geq 0 \tag{11f}$$

Proposed complementarity-based approach

The program $\mathcal{O}_W$ misses the KKT conditions, because the conventional constraint qualifications for nonlinear programming are typically not satisfied in the case of MPCC [Bouza and Still, 2007]. Hence, instead of working with the original problem, the relaxed problem $\mathcal{O}_\epsilon$ is considered:

$$
\begin{aligned}
\mathcal{O}_\epsilon : \quad & \min_{y_p^t} \; -y_p^t f_p^t && \text{(12a)}\\
& \text{s.t.} \quad y_p^t (f_p^t)^2 = K_{nm} \left((\pi_n^t)^2 - (\pi_m^t)^2 \right) && \text{(12b)}\\
& f_p^t = f_{p+}^t - f_{p-}^t && \text{(12c)}\\
& -1 \leq y_p^t \leq 1 && \text{(12d)}\\
& f_{p+}^t (y_p^t + 1) \leq \epsilon && \text{(12e)}\\
& f_{p-}^t (1 - y_p^t) \leq \epsilon && \text{(12f)}
\end{aligned}
$$

The regularized optimization model $\mathcal{O}_\epsilon$ offers several key properties that justify its use in tackling challenging MPCC

Databases

Each of the mentioned databases was selected based on its unique characteristics and the significant contributions it could make to the study.

	Topology	**Connection points**	**Closed loops**	**Problem**
Case 1	9-bus 8-system	1	1	Small system with one loop
Case 2	118-bus 48-system	9	7	Contains several interconnected loops
Case 3	96-bus 63-system	10	0	Fully radial but considers bidirectional flows.

Table 2: Databses used in the study

Experimental setup

In order to establish a baseline for comparison, two alternative methodologies were employed:

- Taylor series approximation [Fodstad et al., 2015].
- Second Order Cone Programming (SOC) [Schwele et al., 2019].

The objective function value for each of the mentioned databases was computed by solving the optimization problem using:

- The IPOPT [Wächter and Biegler, 2005] solver.
- The GEKKO [Beal et al., 2018] package.

Experimental setup

Since understanding and quantifying the inherent errors introduced by any constraint approximation approach supports its real-world pertinence, the considered validation trades off the reached cost function and constraint error values.

$$WE_p^t = |f_p^t - \left(K_{nm}|(\pi_n^t)^2 - (\pi_m^t)^2|\right)^{1/2}|, \quad \forall\ p = (n, m) \in \mathcal{P} \tag{13}$$

Hence, WE_p^t metric explains the inherent sensitivity of tested approaches and validates the significance of their differences.

Results - Case 1

To assess the performance of Weymouth approximation approaches on the 8/9 system, a Monte Carlo experiment estimates the cost function and Weymouth error distributions by solving the optimization problem for one single day one hundred times with uniformly sampled natural gas demands.

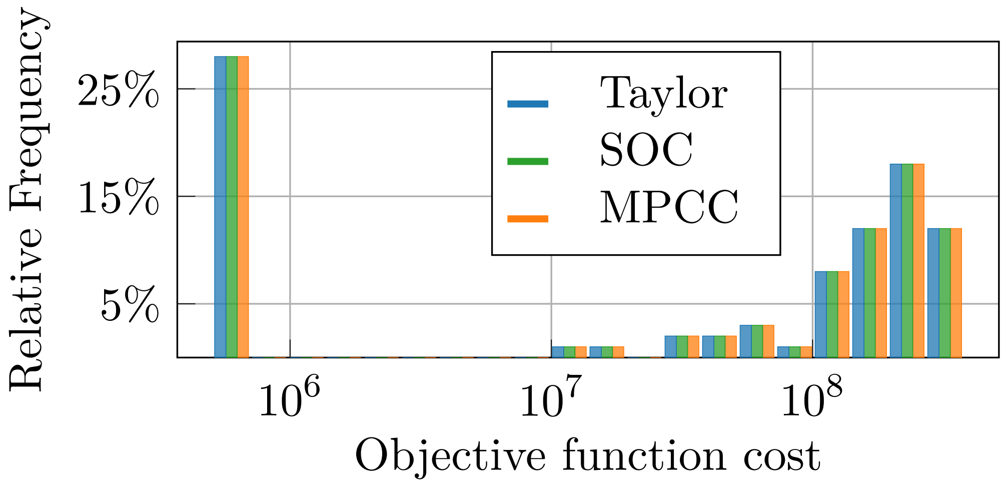

Figure 2: Cost function histogram attained for the Taylor, SOC, and MPCC Weymouth approximation approaches.

Results - Case 1

The boxplot examination reveals significantly lower approximation errors on the proposed complementarity constraints approach over key network arcs.

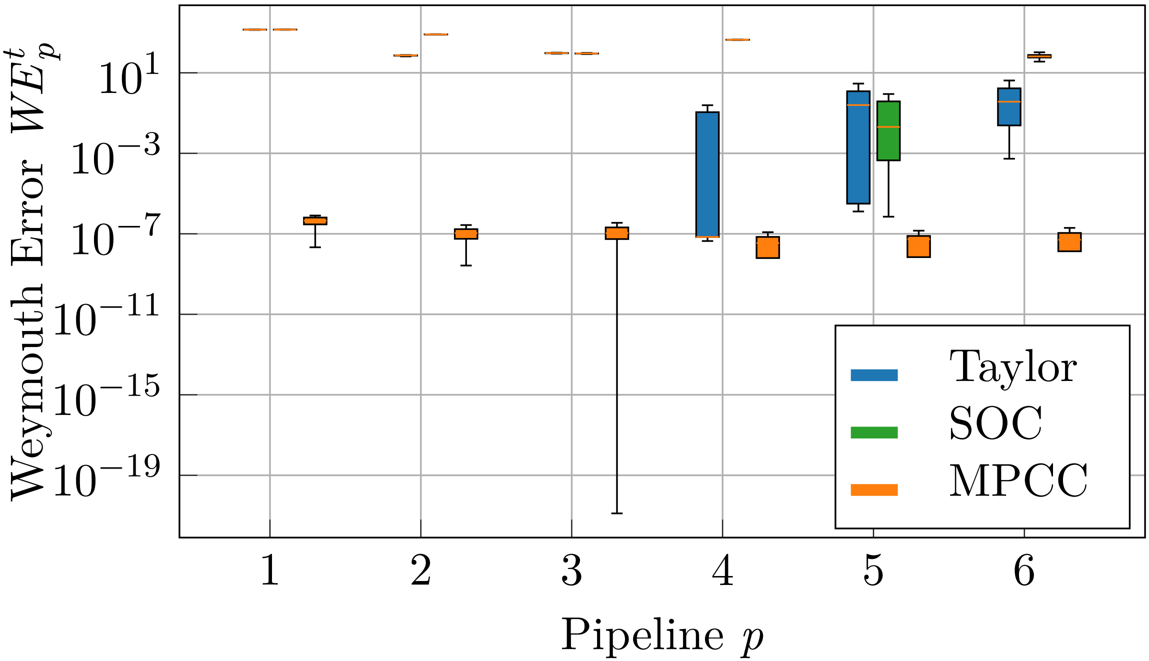

Figure 3: Boxplot of Weymouth error distribution for each pipeline in the 8/9 system attained by contrasted approximation approaches.

Results - Case 2

It is worth noting that both baselines yielded the same objective function values. The consistently positive relative difference indicates that the complementarity constraints formulation always yields larger cost values than Taylor and SOC for the 118/48 system.

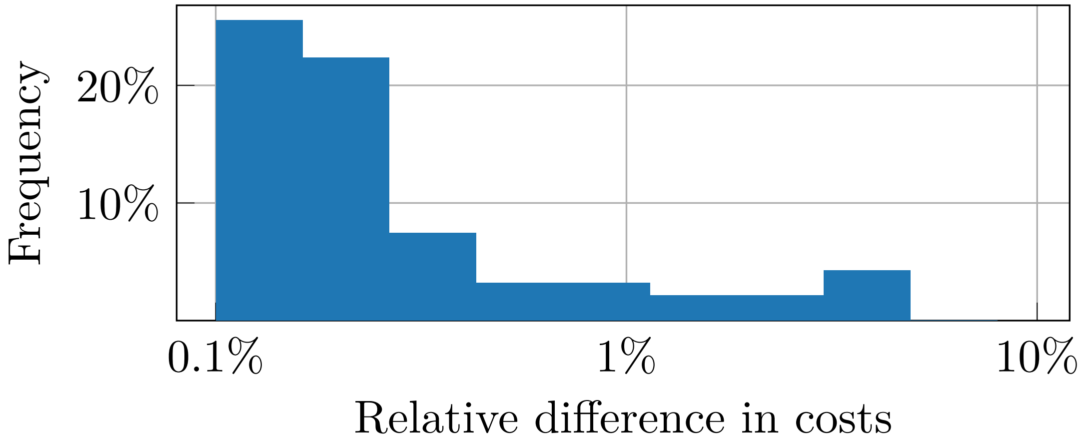

Figure 4: Histogram depicting the relative frequencies of cost differences obtained between MPCC and the other approaches in the 48-node 118-bus system.

Contrarily to cost function analysis, Weymouth approximation results reveal a significant error reduction of about seven orders of magnitude (from 10^1 to 10^{-6}) under the proposed complementarity constraints.

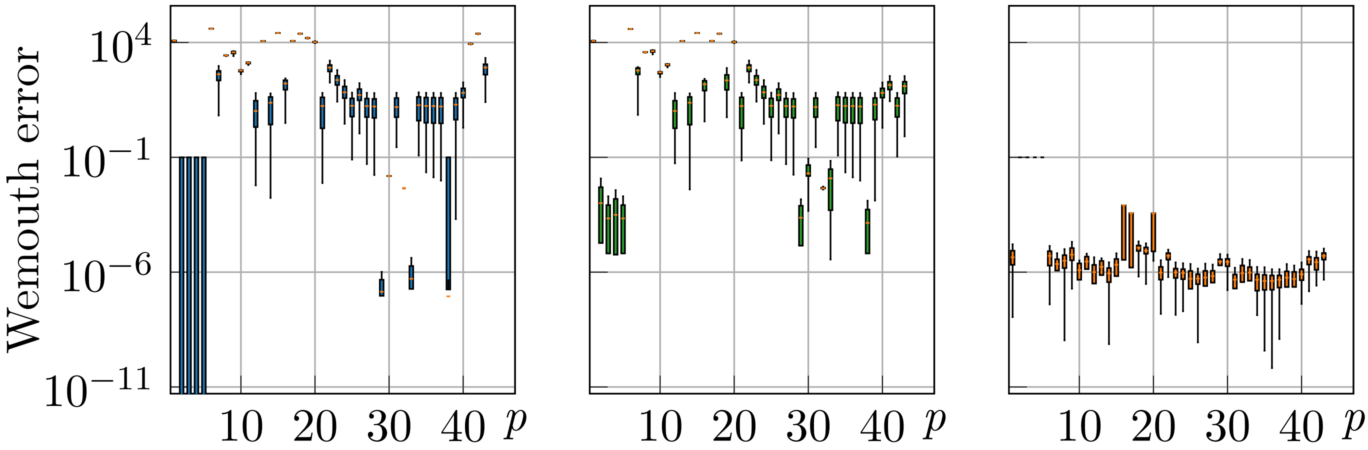

(a) Taylor (b) SOC (c) MPCC

Figure 5: Weymouth approximation errors for each pipeline p reached by Taylor (left), SOC (center), and MPCC (right) approaches in the 118/48 system.

Instead of estimating the distributions of the objective function and Weymouth error as in cases 9/8 and 118/48, the 96/63 case validates the Weymouth approximations in an operation case of ten consecutive days ($|\mathcal{T}| = 10$) with randomly changing gas extraction costs.

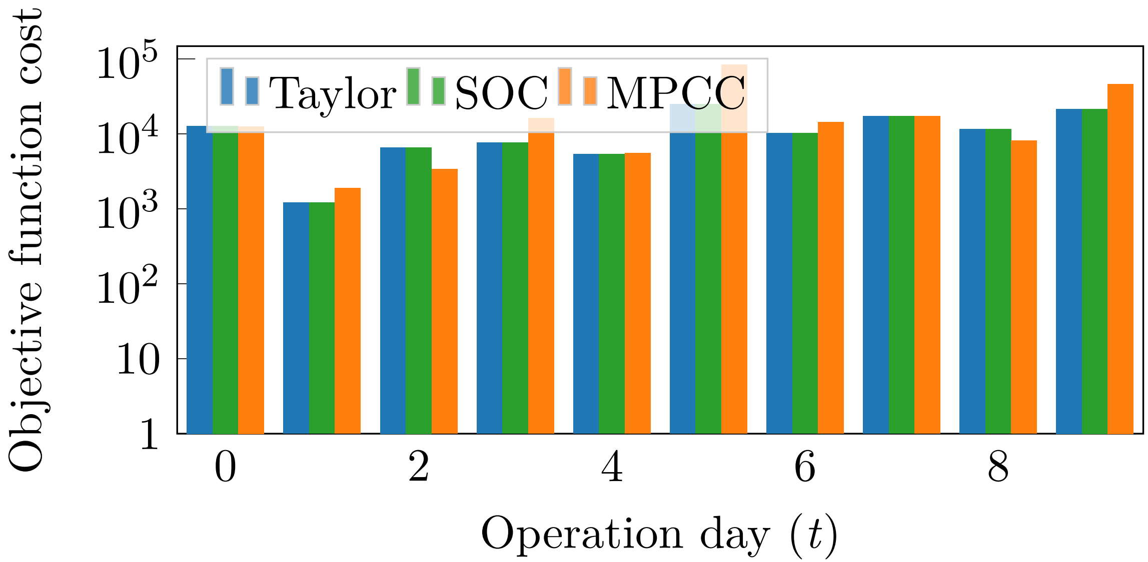

Figure 6: Daily operating cost obtained with each of the approaches in the 63-node 96-bus system.

Results - Case 3

Regarding the Weymouth approximation analysis, the figure presents the error distribution and its relationship with the gas flow and the scheduled day for Taylor, SOC, and MPCC

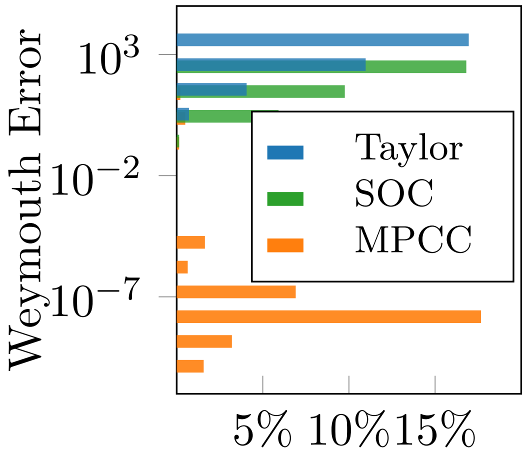

(a) Relative Frequency

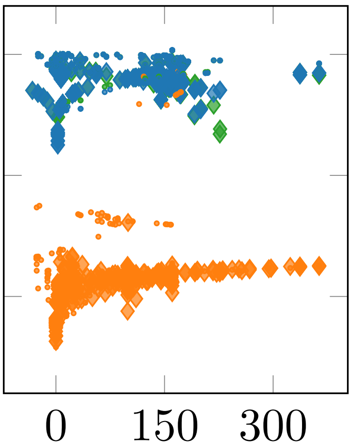

(b) Pipeline flow (f_m^t)

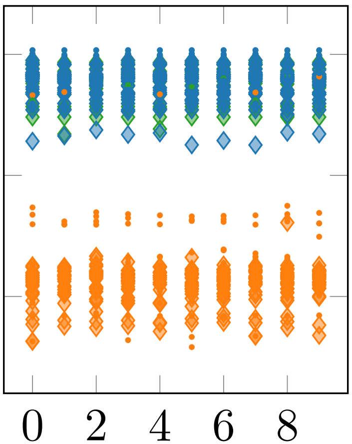

(c) Operation day (t)

Figure 7: Errors in the Weymouth equation expressed in three different formats- general error, error per flow, and error per day.

Physics-Guided Neural Networks

Motivation:

- Traditional neural networks: fit data, ignore physics $\rightarrow$ risk of unrealistic predictions.
- In gas networks, physical constraints (mass balance, pressure-flow laws) are critical.

Physics-Informed Neural Networks (PINNs):

- Incorporate governing equations directly in the loss function.
- Penalize deviations from:
  - **Gas balance constraint** – nodal mass conservation.
  - **Weymouth equation** – relation between flow and pressure differences in pipelines.
- Acts as a *regularizer* for better generalization under uncertainty.

Methodology: Physics-Guided CensNet

Overall loss function:

$$\mathcal{J}(\Theta) = \mathcal{J}_{\text{data}} + \mathcal{J}_{\text{balance}} + \mathcal{J}_{\text{weymouth}}$$

Gas balance loss:

$$\mathcal{J}_{\text{balance}} = \mathbf{T} \cdot \hat{\mathbf{f}}_e - \mathbf{d} + \hat{\mathbf{f}}_n$$

- Enforces nodal inflow = outflow + demand.

Weymouth loss:

$$\mathcal{J}_{\text{weymouth}} = \mathbf{M}_{\mathcal{P}} \left(\hat{\mathbf{f}}_e^{\circ 2} - \mathbf{K} \circ \left(\mathbf{T} \cdot \hat{\boldsymbol{\pi}}^{\circ 2} \right) \right)$$

- Relates squared flows to squared pressure differences.
- Applies only to pipelines (not compressors).

Implementation:

- Built on CensNet architecture from deterministic setup.
- Training data from nonlinear gas network optimization (MPCC).
- Noise (5%–25%) injected to emulate operating uncertainty.

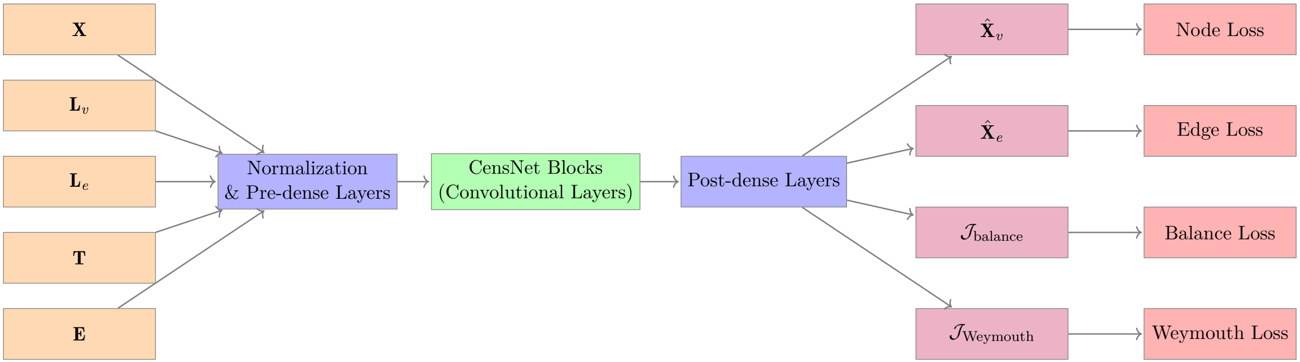

Case Study I: 8-Node Network – Performance Comparison

Method	Node Error	Edge Error	Balance Error	Time (s)
CensNet (N)	0.00 ± 17.99	22.76 ± 15.43	-0.01 ± 17.45	0.86 ± 0.50
CensNet (N+E)	-0.11 ± 18.27	0.22 ± 21.65	-0.12 ± 1.70	0.85 ± 0.50
CensNet (N+E+B)	-0.02 ± 18.00	-0.02 ± 21.30	-0.03 ± 0.90	0.85 ± 0.50
CensNet (N+E+W)	-0.07 ± 17.56	2.60 ± 20.03	-0.07 ± 2.21	0.86 ± 0.50
CensNet (N+E+B+W)	0.05 ± 17.91	0.25 ± 21.14	0.05 ± 1.69	0.85 ± 0.50

Table 3: Performance of CensNet-based models vs. IPOPT benchmark.

- Using only node loss leads to accurate nodal flows but large errors in edge predictions.
- Adding edge loss (**N+E**) reduces edge error from 22.76 to 0.22 and improves global balance.
- Including balance loss (**N+E+B**) further minimizes balance error, achieving best overall consistency.
- Weymouth loss (**N+E+W**) introduces slight trade-offs, slightly increasing edge/balance errors but retaining nodal accuracy.
- All CensNet variants are over an order of magnitude faster than IPOPT, with **N+E+B** offering the best accuracy-speed compromise.

References I

Baumrucker, B., Renfro, J., and Biegler, L. (2008).
Mpec problem formulations and solution strategies with chemical engineering applications.
Computers & Chemical Engineering, 32(12):2903–2913.

Beal, L. D. R., Hill, D. C., Martin, R. A., and Hedengren, J. D. (2018).
Gekko optimization suite.
Processes, 6(8).

Bouza, G. and Still, G. (2007).
Mathematical programs with complementarity constraints: Convergence properties of a smoothing method.
Mathematics of Operations Research, 32(2):467–483.

References II

Duan, J., Liu, F., and Yang, Y. (2022).
Optimal operation for integrated electricity and natural gas systems considering demand response uncertainties.
Applied Energy, 323:119455.

Fodstad, M., Midthun, K. T., and Tomasgard, A. (2015).
Adding flexibility in a natural gas transportation network using interruptible transportation services.
European Journal of Operational Research, 243(2):647–657.

García-Marín, S., González-Vanegas, W., and Murillo-Sánchez, C. (2022).
Mpng: A matpower-based tool for optimal power and natural gas flow analyses.
IEEE Transactions on Power Systems, pages 1–9.

References III

Jiang, T., Yuan, C., Zhang, R., Bai, L., Li, X., Chen, H., and Li, G. (2021).
Exploiting flexibility of combined-cycle gas turbines in power system unit commitment with natural gas transmission constraints and reserve scheduling.
International Journal of Electrical Power & Energy Systems, 125:106460.

Ralph, D. and Wright, S. J. (2004).
Some properties of regularization and penalization schemes for mpecs.
Optimization Methods and Software, 19(5):527–556.

References IV

Schwele, A., Ordoudis, C., Kazempour, J., and Pinson, P. (2019).
Coordination of power and natural gas systems: Convexification approaches for linepack modeling.
In *2019 IEEE Milan PowerTech*, pages 1–6.

Wächter, A. and Biegler, L. T. (2005).
On the implementation of an interior-point filter line-search algorithm for large-scale nonlinear programming.
Mathematical Programming, 106(1):25–57.

Yang, Z., Xie, K., Yu, J., Zhong, H., Zhang, N., and Xia, Q. (2019).
A general formulation of linear power flow models: Basic theory and error analysis.
IEEE Transactions on Power Systems, 34(2):1315–1324.